

# Neutron-Activatable Holmium-Containing Mesoporous Silica Nanoparticles as a Potential Radionuclide Therapeutic Agent for Ovarian Cancer

Anthony J. Di Pasqua<sup>1</sup>, Hong Yuan<sup>2</sup>, Younjee Chung<sup>1</sup>, Jin-Ki Kim<sup>3</sup>, James E. Huckle<sup>1</sup>, Chenxi Li<sup>4</sup>, Matthew Sadgrove<sup>1</sup>, Thanh Huyen Tran<sup>5</sup>, Michael Jay<sup>1</sup>, and Xiuling Lu<sup>5</sup>

<sup>1</sup>Center for Nanotechnology in Drug Delivery, Division of Molecular Pharmaceutics, Eshelman School of Pharmacy, University of North Carolina at Chapel Hill, Chapel Hill, North Carolina; <sup>2</sup>Department of Radiology, University of North Carolina at Chapel Hill, Chapel Hill, North Carolina; <sup>3</sup>College of Pharmacy, Hanyang University, Ansan, Gyeonggi, Republic of Korea; <sup>4</sup>Department of Biostatistics and North Carolina Translational and Clinical Sciences Institute, University of North Carolina at Chapel Hill, Chapel Hill, North Carolina; and <sup>5</sup>Department of Pharmaceutical Sciences, School of Pharmacy, University of Connecticut, Storrs, Connecticut

Mesoporous silica nanoparticles (MSNs) were explored as a carrier material for the stable isotope <sup>165</sup>Ho and, after neutron capture, its subsequent therapeutic radionuclide, <sup>166</sup>Ho (half-life, 26.8 h), for use in radionuclide therapy of ovarian cancer metastasis.

**Methods:** <sup>165</sup>Ho-MSNs were prepared using <sup>165</sup>Ho-acetylacetonate and MCM-41 silica particles, and stability was determined after irradiation in a nuclear reactor (reactor power, 1 MW; thermal neutron flux of approximately  $5.5 \times 10^{12}$  neutrons/cm<sup>2</sup>·s). SPECT/CT and tissue biodistribution studies were performed after intraperitoneal administration of <sup>166</sup>Ho-MSNs to SKOV-3 ovarian tumor-bearing mice. Radiotherapeutic efficacy was studied by using PET/CT with <sup>18</sup>F-FDG to determine tumor volume and by monitoring survival. **Results:** The holmium-MSNs were able to withstand long irradiation times in a nuclear reactor and did not release <sup>166</sup>Ho after significant dilution. SPECT/CT images and tissue distribution results revealed that <sup>166</sup>Ho-MSNs accumulated predominantly in tumors (32.8% ± 8.1% injected dose/g after 24 h; 81% ± 7.5% injected dose/g after 1 wk) after intraperitoneal administration. PET/CT images showed reduced <sup>18</sup>F-FDG uptake in tumors, which correlated with a marked increase in survival after treatment with approximately 4 MBq of <sup>166</sup>Ho-MSNs. **Conclusion:** The retention of holmium in nanoparticles during irradiation and in vivo after intraperitoneal administration as well as their efficacy in extending survival in tumor-bearing mice underscores their potential as a radiotherapeutic agent for ovarian cancer metastasis.

**Key Words:** holmium; mesoporous silica nanoparticle; ovarian cancer; radiotherapeutics; drug delivery

J Nucl Med 2013; 54:1–6

DOI: 10.2967/jnumed.112.106609

**R**apid developments in nanotechnology and nanomaterials have facilitated the creation of multifunctional nanoparticles with targeting, imaging, and therapeutic properties

Received Mar. 26, 2012; revision accepted Jul. 26, 2012.  
For correspondence or reprints contact: Xiuling Lu, University of Connecticut, 69 N. Eagleville Rd., Storrs, CT 06269.  
E-mail: xiuling.lu@uconn.edu  
Published online ■■■■.  
COPYRIGHT © 2013 by the Society of Nuclear Medicine and Molecular Imaging, Inc.

for more effective treatment of cancers, including use as carriers of particle-emitting radionuclides for internal radiation therapy. Internal radiation therapy with radionuclides provides an alternative treatment for metastatic abdominal cancers—epithelial ovarian carcinoma in particular, the leading cause of death from gynecologic malignancies in the developed world. The National Cancer Institute recently released a clinical announcement encouraging the combination of intravenous and intraperitoneal delivery of therapeutic agents for treatment of advanced ovarian cancer (1). Intraperitoneal delivery of β<sup>−</sup> particle-emitting radionuclides has been shown to improve the clinical outcome for patients with peritoneal carcinomatosis (2); however, the toxicity and side effects due to damage to healthy tissues are serious concerns. Colloidal chromic <sup>32</sup>P-phosphate (Phosphocol P 32; Covidien), for example, has been administered intraperitoneally as a palliative treatment of peritoneal metastases in ovarian cancer patients. Accumulation of the radioactive colloidal particles in nontarget tissues due to the broad distribution of particle sizes led to several reported adverse events (3).

An attractive method for producing radioactive particulates for radionuclide therapy is to incorporate stable isotopes within a carrier material and subsequently irradiate it in a neutron flux. This process allows for preparation of the stable isotope carrier without the constraints imposed by short isotope half-lives or the hazards of handling large amounts of radioactivity. For this neutron activation approach to be successful, the carrier material must be able to withstand the neutron irradiation environment, such as in a nuclear reactor, where a high γ-flux can produce high localized heat. Various materials have been used as carriers of stable isotopes with subsequent neutron activation for production of radiotherapeutic particulates. One of the first was glass microspheres with an average diameter of approximately 20–30 μm and containing <sup>89</sup>Y for subsequent activation to <sup>90</sup>Y (4). The high density of these microparticles (3.2 g/cm<sup>3</sup>), which on occasion resulted in particle settling

after intracatheter administration, and the lack of photon emissions by  $^{90}\text{Y}$ , which prevented quantitative imaging, led to the development of other neutron-activatable materials. Microparticles composed of lower-density polymers, including polylactic acid (5–7), alginate (8), and chitosan (9) containing  $^{166}\text{Ho}$ , as well as nanosized carrier materials containing stable  $^{165}\text{Ho}$  for subsequent neutron activation to  $^{166}\text{Ho}$  (10–12), have also been reported.  $^{166}\text{Ho}$  is an attractive radionuclide for radiotherapeutic applications. It emits high-energy  $\beta^-$ -particles with a maximum energy of 1.84 MeV, and its half-life of 26.8 h is amenable for use in radionuclide therapy. In addition,  $^{166}\text{Ho}$  emits 81-keV  $\gamma$ -rays (6.6% photon yield), which allow its biodistribution to be quantified and imaged after administration. However, most of these polymeric carrier materials can withstand only short neutron irradiation times without degrading or aggregating.

Here we report on the incorporation of the lipophilic acetylacetonate complex of  $^{165}\text{Ho}$ ,  $^{165}\text{Ho}(\text{AcAc})_3$ , in mesoporous silica nanoparticles (MSNs), and its subsequent irradiation in a neutron flux to produce particles containing  $^{166}\text{Ho}$  through an (n, $\gamma$ ) reaction. These  $^{166}\text{Ho}$ -MSNs can deliver effective therapeutic doses for treating ovarian cancer metastases after intraperitoneal delivery. Mesoporous silica-type MCM-41, a nanometer-sized assembly of uniform channels stacked in a hexagonal array, has several properties that make it desirable as an efficient drug carrier (13). These include a high surface area, tunable pore structures, and physicochemical stability. The silica nanostructure is capable of adsorbing small molecules such as ibuprofen, acetylsalicylic acid, and famotidine, as well as the anticancer drugs camptothecin and carboplatin (13–15). The cytotoxicity and biocompatibility of mesoporous silica have previously been examined (16–18). The toxicity of mesoporous silica toward cells appears to be related to the adsorptive surface area of the particles (16); however, mice administered 1 mg of mesoporous silica by intraperitoneal injection twice weekly for 2 mo exhibited no unusual responses or behaviors, such as lethargy, weight loss, or immobility, compared with intraperitoneal saline controls (18). In this work, we demonstrated that  $^{166}\text{Ho}$  produced by neutron irradiation of  $^{165}\text{Ho}$ -MSNs was retained in MSNs even after long ( $\leq 18$  h) neutron irradiation times and was not released after dilution. The stability of these  $^{166}\text{Ho}$ -MSNs indicated that the radionuclide would likely be retained within the mesoporous silica matrix after administration to the peritoneal cavity. This is a critical feature, as leakage of  $^{166}\text{Ho}$  from the matrix could result in uptake of the radionuclide in nontarget tissues, for example, bone marrow, and lead to patient morbidity or mortality.

## MATERIALS AND METHODS

### Chemicals

Holmium (III) chloride (99.99%), 2,4-pentanedione ( $\geq 99.9\%$ ), ammonium hydroxide, and mesoporous silica type MCM-41 were purchased from Sigma-Aldrich. All other chemicals were of analytic grade. Holmium acetylacetonate,  $^{165}\text{Ho}(\text{AcAc})_3$ , was prepared as described previously and characterized by  $^1\text{H}$  nuclear

magnetic resonance, electrospray ionization mass spectrometry, and elemental analysis (12).

### Preparation of Holmium-MSNs

To prepare the  $^{165}\text{Ho}$ -MSNs, 10 mg of mesoporous silica type MCM-41 were added to a 15-mL solution containing a 0.5 mg/mL solution of  $^{165}\text{Ho}(\text{AcAc})_3$  in water. The suspension was stirred vigorously for 24 h at room temperature and centrifuged at 1,300g for 20 min. The resulting pellet was washed twice with water and dried in vacuo for 24 h. Inductively coupled plasma-mass spectrometry was used to measure  $^{165}\text{Ho}$  content. Transmission electron microscopy was performed to determine the size of the nanoparticles; their  $\zeta$ -potential in water was measured using a Zetasizer Nano ZS (Malvern).

### Neutron Activation

Dry  $^{165}\text{Ho}$ -MSNs (5–15 mg) were irradiated in the pulsed training assembled reactor (PULSTAR) at North Carolina State University (reactor power, 1 MW; thermal neutron flux of approximately  $5.5 \times 10^{12}$  neutrons/cm $^2$ ·s) for 1–4 or 18 h to produce  $^{166}\text{Ho}$ -MSNs.  $^{166}\text{Ho}$  content was determined by quantifying the 81-keV photons emitted by  $^{166}\text{Ho}$  using a  $\gamma$ -spectrometer that had been calibrated using a National Institute of Standards and Technology-traceable point source. The fast neutron flux was approximately  $8.5 \times 10^{11}$  neutrons/cm $^2$ ·s.

### Stability and Dilution Studies

To determine the percentage of  $^{166}\text{Ho}$  retained by the  $^{166}\text{Ho}$ -MSNs after irradiation and the percentage that remained incorporated after dilution, suspensions containing 4 mg of  $^{166}\text{Ho}$ -MSNs per milliliter in phosphate-buffered saline (PBS; pH 7.4) were diluted with PBS and then passed through 3-kDa molecular weight cutoff filters immediately or after a 24-h incubation at 37°C. The  $^{166}\text{Ho}$  radioactivity in the filtrate was determined using a 2470 Wizard  $\gamma$ -counter (PerkinElmer) and compared with the original activity in the  $^{166}\text{Ho}$ -MSNs.

### Animal Studies

The use of live animals was approved by the University of North Carolina at Chapel Hill Institutional Animal Care and Use Committee, in accordance with the Public Health Service policy on Humane Care and Use of Laboratory Animals, the Amended Animal Welfare Act of 1985, and the regulations of the United States Department of Agriculture.

### In Vivo SPECT/CT and Biodistribution Studies

To determine retention of the particles in the peritoneal cavity after intraperitoneal administration, an ovarian tumor mouse model was used in which athymic (*nu/nu*) mice were injected intraperitoneally with approximately  $7 \times 10^6$  SKOV-3 human ovarian tumor cells. The  $^{166}\text{Ho}$ -MSNs were administered intraperitoneally 2 mo later, after the tumors could be visualized by MRI. Small-animal SPECT/CT was performed 1 and 24 h after intraperitoneal injection of 300  $\mu\text{L}$  of  $^{166}\text{Ho}$ -MSNs ( $\sim 24$  MBq) suspended in 1% carboxymethylcellulose in PBS. Images were acquired using an eXplore speCZT system (GE Healthcare) with a mouse multislit collimator and reconstructed using a 70- to 90-keV energy window to detect the 81-keV photons emitted from  $^{166}\text{Ho}$  (12). The distribution of  $^{166}\text{Ho}$  in various organs in SKOV-3 ovarian tumor-bearing mice at 1 h, 24 h, and 1 wk after intraperitoneal injection of  $^{166}\text{Ho}$ -MSNs was then determined. The mass of each organ was measured, and the  $^{166}\text{Ho}$  content was quantified using a 2470 Wizard  $\gamma$ -counter. Autoradiography was conducted on tumor sections to further investigate the spatial distribution of  $^{166}\text{Ho}$  particles within the tumors. Tumor tissues removed from

mice 24 h after intraperitoneal injection of the  $^{166}\text{Ho}$ -MSNs were cryosectioned at a thickness of 14  $\mu\text{m}$  using a Leica 1850 system. Tumor sections were exposed to a storage phosphor screen (GE Healthcare), and then the phosphor screen was scanned using a digital phosphor imager (Cyclone Plus; PerkinElmer).

### Efficacy Study

Tumor growth was monitored in vivo over time using PET/CT after administration of  $^{18}\text{F}$ -FDG. Ovarian tumor-bearing mice were administered 2 mg of nonirradiated  $^{165}\text{Ho}$ -MSNs or  $^{166}\text{Ho}$ -MSNs ( $\sim 4$  MBq) in 200  $\mu\text{L}$  of 1% carboxymethylcellulose in PBS via intraperitoneal injection ( $n = 5$ ).  $^{18}\text{F}$ -FDG PET/CT was performed before (day 0) and at 6, 13, and 20 d after injection of the therapeutic or control particles. Images were acquired using a small-animal PET/CT system (eXplore Vista/CT model; GE Healthcare). Food was withdrawn at least 2 h before  $^{18}\text{F}$ -FDG was dosed; each mouse was anesthetized with isoflurane (1.5%) mixed with oxygen. The mice were administered 7.4 MBq of  $^{18}\text{F}$ -FDG via the tail vein and were kept warm on a heating pad before being moved to the PET/CT scanner. CT was performed initially to obtain an anatomic reference and for signal attenuation correction. A static PET image acquisition was started 30 min after  $^{18}\text{F}$ -FDG injection and continued for 10 min. Images were reconstructed using 2-dimensional ordered-subsets expectation maximization with scatter correction, random correction, and attenuation correction. A standardized uptake value was calculated on the basis of the calibrated counts, the injected dose, and the animal body weight. Images were analyzed using the region-of-interest-based method. For each animal, tumor regions were manually labeled at similar anatomic positions at each time point. The maximum standardized uptake value in the region of interest at various time points relative to that at day zero was calculated as the percentage  $^{18}\text{F}$ -FDG uptake.

### Survival Study

Twenty days after intraperitoneal implantation of  $15 \times 10^6$  SKOV-3 human ovarian tumor cells, the tumor-bearing mice were injected intraperitoneally with a single dose of  $^{166}\text{Ho}$ -MSNs (0.33 mg;  $\sim 4$  MBq), an equivalent amount of  $^{166}\text{Ho}(\text{AcAc})_3$ , or 0.33 mg of stable  $^{165}\text{Ho}$ -MSNs in 400  $\mu\text{L}$  of 1% carboxymethylcellulose in PBS ( $n = 12$  per treatment group). An additional 14 mice that received no treatment served as a control group. The mice were euthanized if weight loss was greater than 10% over a 3-d period; if weight loss was greater than 20% over the course of the study, or if tumor growth interfered with mobility, such as in mice with obvious ascites. One-sided Fisher exact tests were used to compare the fraction of mice that had survived for 73 d after implantation among the 4 treatment groups.

## RESULTS

$^{165}\text{Ho}$ -MSNs were prepared by the addition of mesoporous silica type MCM-41 to a concentrated solution of  $^{165}\text{Ho}(\text{AcAc})_3$  in water followed by vigorous stirring for 24 h at room temperature. This approach is common for incorporating small molecules into MSNs (13–15). On the basis of TEM images, these nanoparticles were estimated to be approximately 80–100 nm in diameter, and they had a  $\zeta$ -potential in water of  $-49.2 \pm 6.0$  mV. Dry  $^{165}\text{Ho}$ -MSNs were then irradiated in the PULSTAR nuclear reactor for 1–18 h to produce  $^{166}\text{Ho}$ -MSNs. The amount of holmium that had been adsorbed by mesoporous silica, determined by quantifying the 81-keV photons

emitted by  $^{166}\text{Ho}$ , was  $17.8\% \pm 1.4\%$  of the weight of the holmium-MSNs. This result was corroborated by inductively coupled plasma mass spectrometry detecting for  $^{165}\text{Ho}$ . Because of the high  $^{166}\text{Ho}$  content in the nanoparticles, significant levels of radioactivity were obtained after neutron irradiation. For example, irradiation of 10.7 mg of the particles in a thermal neutron flux of approximately  $5.5 \times 10^{12}$  neutrons/cm $^2$ -s for 2.2 h yielded 129.5 MBq of  $^{166}\text{Ho}$ . The dilution studies showed that after 1 or 18 h of irradiation, approximately 100% of the holmium was retained by the  $^{166}\text{Ho}$ -MSNs and that there was essentially no release of radioactivity from these particles after incubation at 37°C for 24 h or after 10- and 100-fold dilutions in PBS followed by incubation at 37°C for 24 h.

Small-animal SPECT/CT images of SKOV-3 ovarian tumor-bearing mice 1 and 24 h after intraperitoneal injection of the  $^{166}\text{Ho}$ -MSNs showed that the particles accumulated predominantly in tumors (Fig. 1A), which were clearly visible in the animal after sacrifice (Fig. 1B). A large dose ( $\sim 24$  MBq) was required for high-resolution SPECT because of the low photon yield of  $^{166}\text{Ho}$ . The distribution of  $^{166}\text{Ho}$  in SKOV-3 ovarian tumor-bearing mice at selected time points after intraperitoneal injection of  $^{166}\text{Ho}$ -MSNs was then determined. The percentage injected dose of  $^{166}\text{Ho}$  per gram in various organs 1 h, 24 h, and 1 wk after administration is shown in Figure 2A. After 24 h,  $32.8\% \pm 8.1\%$  injected dose/g of the  $^{166}\text{Ho}$ -MSNs had accumulated in tumors. Tumor accumulation in mice treated with  $^{166}\text{Ho}$ -MSNs increased to  $81\% \pm 7.5\%$  injected dose/g after 1 wk, which was more than 12 times that in any other organ (i.e., liver, spleen). To further investigate the spatial distribution of  $^{166}\text{Ho}$  particles within the tumors, autoradiography images of tumor sections were superimposed on photographs of the same tumor slices obtained from mice 24 h after intraperitoneal administration of the  $^{166}\text{Ho}$ -MSNs (Fig. 2B). Most tumor slices revealed the presence of radioactivity on their surfaces, but some had radioactivity distributed throughout the entire tumor.

The tumor uptake and biodistribution studies were followed by a pilot efficacy study in which tumor growth was monitored by measuring energy consumption using the radiofluorinated glucose analog  $^{18}\text{F}$ -FDG and PET/CT after the administration of  $^{166}\text{Ho}$ -MSNs or nonirradiated  $^{165}\text{Ho}$ -MSNs to ovarian tumor-bearing mice. Uptake of  $^{18}\text{F}$ -FDG has been shown to be useful for determining the volume of highly metabolically active tumors (19). The standardized uptake value associated with  $^{18}\text{F}$ -FDG measured in tumors of mice treated with  $^{166}\text{Ho}$ -MSNs decreased over time, whereas no change was observed in mice administered the control, nonirradiated  $^{165}\text{Ho}$ -MSNs (Fig. 3). Over the 20-d observation period, the active tumor volume of the mice administered  $^{166}\text{Ho}$ -MSNs was significantly reduced ( $P < 0.05$ ), whereas the nonirradiated control particles failed to reduce the volume of any tumors.

A survival study was subsequently performed to confirm the results of the pilot efficacy study. The survival of animals that were administered  $^{166}\text{Ho}$ -MSNs was compared with the survival of mice that had been administered  $^{166}\text{Ho}(\text{AcAc})_3$  or the nonradioactive particles ( $^{165}\text{Ho}$ -MSNs) 20 d after tumor

RGB

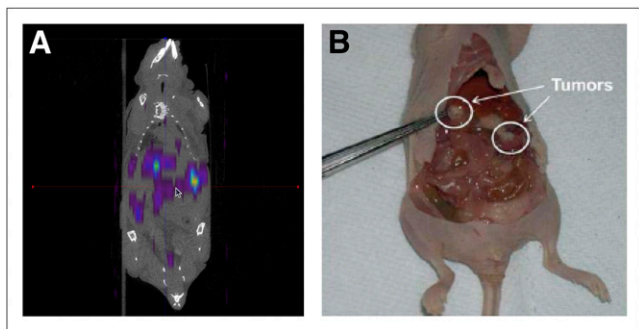


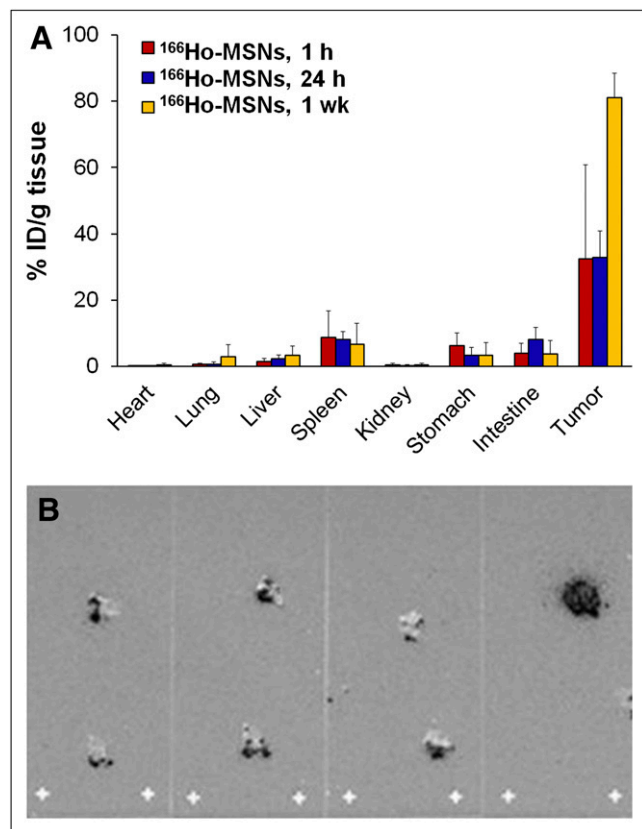
**FIGURE 1.** SKOV-3 ovarian tumor-bearing mouse after intraperitoneal injection of  $^{166}\text{Ho}$ -MSNs. (A) SPECT/CT image obtained 1 h after treatment. (B) Photograph of dissected mouse 24 h after treatment.

implantation, as well as with mice that had received no treatment. All mice that had not died or been euthanized were considered to have their survival times right-censored at day 73. The number of surviving animals was greatest in the group that was treated with  $^{166}\text{Ho}$ -MSNs (91.7%), followed by animals treated with  $^{166}\text{Ho}(\text{AcAc})_3$  (66.7%). The number of surviving animals after treatment with stable  $^{165}\text{Ho}$ -MSNs was similar to that of the no-treatment group [Fig. 4] (33.3% and 35.7%, respectively, Fig. 4). One-sided Fisher exact tests showed that the survival fraction of mice in the  $^{166}\text{Ho}$ -MSN group was significantly higher than that in either the  $^{165}\text{Ho}$ -MSN or the no-treatment group ( $P = 0.005$ ). The number of mice surviving to day 73 was not significantly greater among those treated with  $^{166}\text{Ho}(\text{AcAc})_3$  than among those treated with  $^{165}\text{Ho}$ -MSNs ( $P = 0.110$ ) or receiving no treatment ( $P = 0.119$ ). However, the greater fractional survival of the mice treated with  $^{166}\text{Ho}$ -MSNs than of mice treated with  $^{166}\text{Ho}(\text{AcAc})_3$  did not achieve significance ( $P = 0.158$ ). These results, coupled with the long survival times observed for untreated mice in this tumor model, indicate that larger group sizes are required to establish statistically significant differences among all groups.

## DISCUSSION

Although radionuclides have been used therapeutically for several decades, the chief concern has been their accumulation in nontarget tissues. This problem can be controlled to some degree by administering the therapeutic radionuclides in micro- and nanoparticulate carriers. Incorporating hazardous radionuclides in these carriers can be challenging; the process may not be amenable to handling large amounts of radioactivity and may be constrained by decay of the radionuclide, particularly those with relatively short half-lives. Neutron activation of particulates containing stable isotopes as a means of producing carriers of radioactive isotopes can overcome these limitations but produces new challenges as well. Most of these challenges—for example, stability during neutron irradiation and retention of the radionuclide in the carrier after administration—relate to the material aspects of the carriers.

The work described here focused on the use of a nano-carrier material, mesoporous silica type MCM-41, that possesses many desirable properties as a carrier for therapeutic radionuclides produced by neutron activation. MCM-41 has a large surface area ( $\sim 1,000 \text{ m}^2/\text{g}$ ), which is ideal for adsorption of small molecules (13) such as  $^{165}\text{Ho}(\text{AcAc})_3$ , and, as shown here, can withstand long irradiation times in a nuclear reactor. These studies demonstrated the flexibility in producing  $^{166}\text{Ho}$ -MSNs with different amounts of radioactivity by varying neutron irradiation times. High-activity particles were produced in which the cumbersome process of handling large amounts of a hazardous radionuclide was avoided during the manufacture of radiotherapeutic particles. The use of long irradiation times in reactors with higher neutron flux densities enables the production of particles with higher specific activity. When this technology is translated to humans, it is expected that a therapeutic amount of radioactivity will be delivered with a relatively small mass of particles, comparable to  $^{90}\text{Y}$  glass microspheres, up to 120 mg of which may be used in the treatment of hepatocellular carcinoma (20). Furthermore,  $^{166}\text{Ho}$ -MSNs were stable on dilution, eliminating concerns about the effect of dilution in



RGB

**FIGURE 2.** Biodistribution of  $^{166}\text{Ho}$ -MSNs in SKOV-3 ovarian tumor-bearing mice ( $n \geq 4$ ). (A) Percentage injected dose (ID) per gram of  $^{166}\text{Ho}$  in organs of mice at 1 h, 24 h, or 1 wk after intraperitoneal injection of  $^{166}\text{Ho}$ -MSNs. (B) Autoradiography image (dark color) superimposed on image of tumor slices (gray color) from mouse treated with  $^{166}\text{Ho}$ -MSNs for 24 h. Increased pixel intensity (darker color) represents increased radioactivity of  $^{166}\text{Ho}$  in tumor slices.

RGB

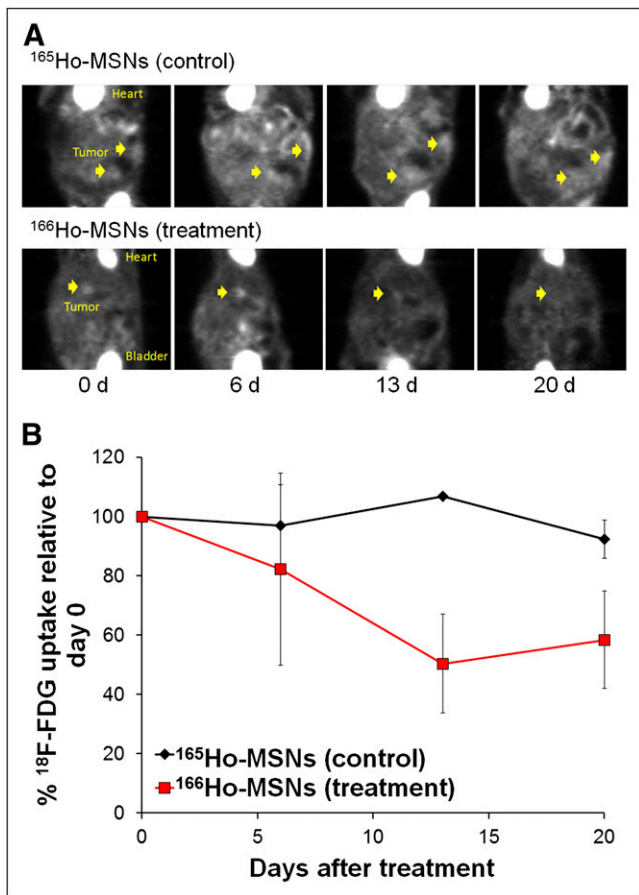
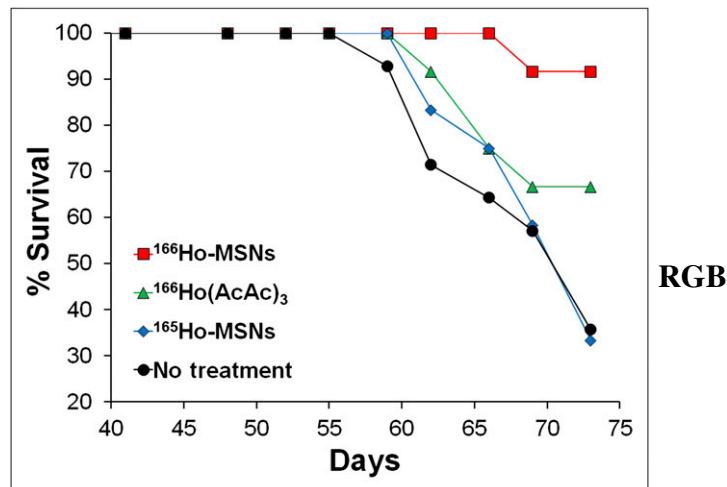


**FIGURE 3.** Efficacy of  $^{166}\text{Ho}$ -MSNs. (A)  $^{18}\text{F}$ -FDG PET/CT images in SKOV-3 ovarian tumor-bearing mice before (0 d) intraperitoneal injection of nonirradiated  $^{165}\text{Ho}$ -MSNs (control) or  $^{166}\text{Ho}$ -MSNs and at 6, 13, and 20 d after injection. (B) Tumor uptake of  $^{18}\text{F}$ -FDG relative to day 0 as function of time after injection.

the peritoneal cavity on the stability of  $^{166}\text{Ho}$  retention by MSNs after intraperitoneal injection.

SPECT/CT images and tissue distribution results revealed that  $^{166}\text{Ho}$ -MSNs accumulated predominantly in tumors after intraperitoneal administration. Tumor accumulation of  $^{166}\text{Ho}$ -MSNs after 24 h was more than twice that of  $^{166}\text{Ho}(\text{AcAc})_3$ . Interestingly, there were no tumor-targeting ligands attached to the surface of the  $^{166}\text{Ho}$ -MSNs; even so, the tumor accumulation was exceptionally high and increased with time. The results indicate that  $^{166}\text{Ho}$ -MSNs particles may have a strong affinity for the tumor surface or may be taken up by tumor cells. The mechanism by which these particles are taken up by tumors is under further investigation.

From the  $^{18}\text{F}$ -FDG/PET study, it is clear that treatment with  $^{166}\text{Ho}$ -MSNs caused rapid reduction in tumor volume, followed by stabilization. This pattern correlated with a marked increase in survival after treatment with approximately 4 MBq of  $^{166}\text{Ho}$ -MSNs, compared with groups receiving  $^{165}\text{Ho}$ -MSNs or no treatment. It was anticipated that survival of tumor-bearing animals receiving  $^{166}\text{Ho}(\text{AcAc})_3$  would be greater than that of animals receiving



RGB

**FIGURE 4.** Survival of ovarian tumor-bearing mice after intraperitoneal administration of nonirradiated  $^{165}\text{Ho}$ -MSNs,  $^{166}\text{Ho}$ -MSNs,  $^{166}\text{Ho}(\text{AcAc})_3$ , or no treatment. All administrations were 20 d after intraperitoneal implantation of  $15 \times 10^6$  SKOV-3 human ovarian tumor cells.

no treatment or treatment with nonradioactive MSNs but would be less than that of animals receiving radioactive MSNs. Figure 4 supports this trend, although the differences in the numbers of surviving animals in each of these treatment groups were not statistically significant. However, the high survival (91.7%) 73 d after tumor implantation demonstrated a beneficial effect of the  $^{166}\text{Ho}$ -MSNs particles and suggested that efficacy would be further improved if a multiple-dose regimen of  $^{166}\text{Ho}$ -MSNs were used.

The absorbed radiation dose from  $^{166}\text{Ho}$  was estimated on the basis of the average uptake of radioactivity in each tumor, assuming that activity accumulated mainly in the tumor center. With an intraperitoneal injection of about 4 MBq of  $^{166}\text{Ho}$ -MSNs, the average uptake of activity in each tumor (mean diameter, 4 mm) was approximately 0.3 MBq at 24 h after injection, based on the biodistribution results. It has been reported that for  $^{166}\text{Ho}$ , 90% of the radiation dose is delivered to tissue within 2.1 mm of the source (21,22). Assuming  $^{166}\text{Ho}$ -MSNs were distributed in the tumor center, most of the energy from  $^{166}\text{Ho}$  (average, 689 keV; maximum, 1.84 MeV) could be deposited within a 4-mm tumor. The total absorbed radiation dose in each tumor can thus be calculated by the total energy deposition divided by tumor mass, resulting in an average of 134.7 Gy in a 4-mm-diameter tumor, which is sufficient for a tumor killing effect. The assumption of central distribution of  $^{166}\text{Ho}$  within tumor tissue overestimates the actual radiation dose in cases with activity spreading throughout the tumor or at the tumor edge. Nevertheless, an approximate estimation was provided of the maximum radiation dose from a small number of  $^{166}\text{Ho}$  particles. More accurate dosimetry analysis is being conducted using Monte Carlo simulations based on actual activity distributions from autoradiography or SPECT images.

## CONCLUSION

Radiotherapeutic nanoparticles were produced by a neutron activation process that allows limited handling of radioactive materials. The  $^{166}\text{Ho}$  that was produced was retained in MSNs after long reactor irradiation times and was not released after dilution. Tomographic images demonstrated that most of the  $^{166}\text{Ho}$ -MSNs administered to ovarian tumor-bearing mice were retained in the peritoneal cavity and selectively accumulated in the tumors. PET/CT with  $^{18}\text{F}$ -FDG demonstrated that the  $^{166}\text{Ho}$ -MSNs reduced tumor volume, which correlated with a marked increase in survival. Dosimetry calculations support the use of  $^{166}\text{Ho}$ -MSNs for treating ovarian cancer metastases in humans.

## DISCLOSURE STATEMENT

The costs of publication of this article were defrayed in part by the payment of page charges. Therefore, and solely to indicate this fact, this article is hereby marked "advertisement" in accordance with 18 USC section 1734.

## ACKNOWLEDGMENTS

Special thanks are given to Scott Lassell at the Nuclear Reactor Program at North Carolina State University and the Small Animal Imaging Core at UNC. We gratefully acknowledge support from the National Center for Research Resources and the University Cancer Research Fund at UNC Chapel Hill (award UL1RR025747), as well as a Benedict Cassen Postdoctoral Fellowship from the Education and Research Foundation of the Society of Nuclear Medicine and Molecular Imaging. No other potential conflict of interest relevant to this article was reported.

## REFERENCES

1. Intraperitoneal therapy for ovarian cancers. National Cancer Institute Web site. Available at: <http://www.cancer.gov/clinicaltrials/conducting/developments/ipchemodigest/Pagel>. Accessed October 19, 2012.
2. Spencer TR, Marks RD, Fenn JO, Jenrette JM, Lutz MH. Intraperitoneal P-32 after negative second-look laparotomy in ovarian carcinoma. *Cancer*. 1989;63:2434–2437.
3. Phosphocol P 32 (chromic phosphate P 32 suspension). U.S. Food and Drug Administration Web site. Available at: [http://www.fda.gov/Safety/MedWatch/](http://www.fda.gov/Safety/MedWatch/SafetyInformation/SafetyAlertsforHumanMedicalProducts/ucm094958.htm)

4. Tian JH, Xu BX, Zhang JM, Dong BW, Liang P, Wang XD. Ultrasound-guided internal radiotherapy using yttrium-90-glass microspheres for liver malignancies. *J Nucl Med*. 1996;37:958–963.
5. Mumper RJ, Yun Ryo U, Jay MJ. Neutron-activated holmium-166-poly (L-lactic acid) microspheres: a potential agent for the internal radiation therapy of hepatic tumors. *J Nucl Med*. 1991;32:2139–2143.
6. Zielhuis SW, Nijssen JFW, Seppenwoolde JH, et al. Long-term toxicity of holmium loaded poly(L-lactic acid) microspheres in rats. *Biomaterials*. 2007;28:4591–4599.
7. Bult W, Seevinck PR, Krijger GC, et al. Microspheres with ultrahigh holmium content for radioablation of malignancies. *Pharm Res*. 2009;26:1371–1378.
8. Zielhuis SW, Seppenwoolde JH, Bakker CJG, et al. Characterization of holmium loaded alginate microspheres for multimodality imaging and therapeutic applications. *J Biomed Mater Res A*. 2007;82:892–898.
9. Kim JK, Han KH, Lee JT, et al. Long-term clinical outcome of phase IIb clinical trial of percutaneous injection with holmium-166/chitosan complex (Milican) for the treatment of small hepatocellular carcinoma. *Clin Cancer Res*. 2006;12:543–548.
10. Hamoudeh M, Fessi H, Salim H, Barbos D. Holmium-loaded PLLA nanoparticles for intratumoral radiotherapy via the TMT technique: preparation, characterization, and stability evaluation after neutron irradiation. *Drug Dev Ind Pharm*. 2008;34:796–806.
11. Bult W, Varkevisser R, Soulimani F, et al. Holmium nanoparticles: preparation and *in vitro* characterization of a new device for radioablation of solid malignancies. *Pharm Res*. 2010;27:2205–2212.
12. Di Pasqua AJ, Huckle JE, Kim JK, et al. Preparation of neutron-activatable holmium nanoparticles for the treatment of ovarian cancer metastases. *Small*. 2012;8:997–1000.
13. Vallet-Regi M, Balas F, Arcos D. Mesoporous materials for drug delivery. *Angew Chem Int Ed Engl*. 2007;46:7548–7558.
14. Zeng W, Qian XF, Zhang YB, Yin J, Zhu ZK. Organic modified mesoporous MCM-41 through solvothermal process as drug delivery system. *Mater Res Bull*. 2005;40:766–772.
15. Di Pasqua AJ, Wallner S, Kerwood DJ, Dabrowiak JC. Adsorption of the Pt<sup>2+</sup> anticancer drug carboplatin by mesoporous silica. *Chem Biodivers*. 2009;6:1343–1349.
16. Di Pasqua AJ, Sharma KK, Shi YL, et al. Cytotoxicity of mesoporous silica nanomaterials. *J Inorg Biochem*. 2008;102:1416–1423.
17. Hudson SP, Padera RF, Langer R, Kohane DS. The biocompatibility of mesoporous silicates. *Biomaterials*. 2008;29:4045–4055.
18. Lu J, Liong M, Li Z, Zink JL, Tamanoi F. Biocompatibility, biodistribution, and drug-delivery efficiency of mesoporous silica nanoparticles for cancer therapy in animals. *Small*. 2010;6:1794–1805.
19. Miller TR, Grigsby PW. Measurement of tumor volume by PET to evaluate prognosis in patients with advanced cervical cancer treated by radiation therapy. *Int J Radiat Oncol Biol Phys*. 2002;53:353–359.
20. Ho S, Lau JWY, Leung TWT. Intrahepatic  $^{90}\text{Y}$ -microspheres for hepatocellular carcinoma. *J Nucl Med*. 2001;42:1587–1589.
21. Tandon P, Malpani BL, Venkatesh M, Bhatt BC. Estimation of radiation dose at various depths for commonly used radionuclides in radiosynoviothrosis in a tissue equivalent material. *Med Phys*. 2006;33:2744–2750.
22. Johnson LS, Yanch JC. Absorbed dose profiles for radionuclides of frequent use in radiation synovectomy. *Arthritis Rheum*. 1991;34:1521–1530.